N88-17587

NAVIER-STOKES CALCULATIONS AND TURBULENCE MODELING IN THE TRAILING EDGE REGION OF A CIRCULATION CONTROL AIRFOIL

by

John R. Viegas and Morris W. Rubesin
NASA Ames Research Center

and

Robert W. MacCormack*
Stanford University

Introduction

The accurate prediction of turbulent flows over curved surfaces in general and over the trailing edge region of circulation control airfoils in particular will require the coupled efforts of turbulence modelers, numerical analysts and experimentalists. In this paper the purpose of our research program in this area will be described (see Fig. 1). Then, the influence on turbulence modeling of the flow characteristics over a typical circulation control wing will be discussed. Next, the scope of this effort to study turbulence in the trailing edge region of a circulation control airfoil will be presented. This will be followed by a brief overview of the computation scheme, including the grid, governing equations, numerical method, boundary conditions and turbulence models applied to date. Then, examples of applications of two algebraic eddy viscosity models (and variants thereof) to the trailing edge region of a circulation control airfoil will be presented. The results from the calculations will be summarized, and conclusions drawn based on the examples. Finally, the future directions of the program will be outlined.

Objective

The overall objective of this research program, summarized in Fig. 2, is to develop an improved turbulence model to permit accurate computation of the flow fields about circulation control wings over a range of flight conditions and trailing edge configurations.

The approach is both computational and experimental. Numerical solutions of flow over circulation control airfoils for various geometries and turbulence models will be used to test, develop and improve the turbulence models for these flows. The experimental program will perform companion experiments over these same flow conditions/geometries to measure turbulence quantities needed to understand these complex flows. The measured results will be used to guide and verify the turbulence modeling over a range of Mach numbers and for various trailing edge configurations.

The present paper will only address the computational part of this program.

Modeling Aspects

The flow about the trailing edge region of a circulation control wing presents a challenging environment to turbulence modelers. Some of the important modeling aspects under these flow conditions, as summarized in Fig. 3, are:

1. The flow is three-dimensional due to the wing having a finite aspect ratio and to being yawed relative to the mean motion.

2

2. The flow within the boundary layer of a yawed wing experiences large changes in the angles of skewing, (Spaid and Keener, 1986.)

3. Compressibility effects occur in transonic flow regimes and in underexpanded jets. Current Navier-Stokes solvers handle these effects quite well.

4. Multiple streams with different turbulence intensity and length scales merge at the jet and separation points. This requires significant modification to current mixing length models in these regions.

5. The flows experience extreme streamwise curvature way beyond conditions on which usual curvature corrections are based.

6. The flows can experience large regions of separation. Predicting the location of the separation point and the extent of separation correctly is a critical test of a turbulence model. These are also important parameters in the description of the performance of a circulation control airfoil. Unfortunately most turbulence models have difficulty in regimes of large separation.

Current Activities

Current activities have stressed development of a two-dimensional numerical code to permit testing a variety of existing turbulence models and to accept new models likely to be required. This code solves the Reynolds-averaged Navier-Stokes equations in the trailing edge region of a circulation control airfoil. The computational domain is confined to the trailing edge region of the airfoil to emphasize those aspects of this region on the turbulence model (see above) and to allow for high resolution with relatively few mesh points. This latter feature may be very important when complex turbulence models, that are costly in computer time, are tested and developed.

To date only algebraic models of turbulence have been incorporated in the code. These are the well known models developed by Baldwin and Lomax (Baldwin-Lomax, 1978) and by Cebeci and Smith (Cebeci-Smith, 1974). These models, plus modifications, will be shown later.

Computational Domain

For this workshop, the code was used to calculate the flow in the trailing edge region of circulation control wing experiment that was performed at NASA Ames Research Center.

This experiment was the result of a cooperative effort between McDonnell-Douglas and Ames and is reported in another paper of this workshop (Spaid and Keener, 1986). It was chosen for computation because it provided an opportunity for easy access to the experimentors. This wing had a 10 inch chord and was swept back 45°. The case chosen for calculation purposes was one in which the free stream Mach number and the jet pressure ratio were 0.426 and 1.4, respectively.

The sketch on the left side of Fig. 4 shows a typical circulation control wing yawed relative to the mean flow. Shown also is a plane parallel to the mean flow as it crosses the wing. Experimental evidence shows that in the Spaid-Keener experiment the resultant velocity vector in the boundary layer on the top wing surface turned (or skewed) inboard to become nearly parallel to the jet at the surface. In anticipation of eventually obtaining data in the future for an unyawed wing, it was decided to perform the two-dimensional calculations in a plane containing the mean jet velocity vector. It was felt that for such a two-dimensional calculation it would be more important to work in the characteristic plane of the jet and the near-wall flow on the top surface than in the mean flow plane. This satisfied the primary purpose of this work, namely, to test the numerical behavior and the simple turbulence models of the code with typical geometrical and flow parameters. For this limited objective the free stream Mach number and jet pressure are not altered from their swept wing values.

The sketch on the right hand side of figure 4 shows the computational domain in relation to a cross section of the wing. The plane of the figure is normal to the trailing edge of the wing. The wing chord is about 10 inches long and the radius of the computational domain is about 2 feet in length. The vertical boundary for the incoming flow at the top of the airfoil is located at the jet slot. The vertical boundary at the bottom of the airfoil is located at X/C = 0.899, a point where experimental data was available.

The far field grid used in the calculations is shown in Fig. 5. It extends two feet from the body (about 50 tip radii). The outer boundary is circular for the most part. The circles are offset from the center of radius for the trailing edge to provide a vertical location for boundary conditions at the inflow boundaries. The grid spacing stretches exponentially away from the body. A very fine grid is used next to the body to resolve the region where viscous effects are important. The dark region next to the body represents the compressed scales of the fine mesh region which are not resolvable on the scale of this figure. The dark vertical stripe results from the extension of the fine scales, in the flow direction adjacent to the surface, vertically whereas the remainder of the grid is extended radially. The distances on this and subsequent figures are given in feet.

A magnified view of the grid, to show the near field, is presented in Fig. 6. On the scale of this figure the dark vertical stripe on Fig. 5 is seen to blend smoothly with the grid surrounding the trailing edge at the body. Again, the dark band near the surface represents grid spacings that still cannot be resolved at this scale. A total of 61 grid points were used normal to the surface and 65 grid points were used in the circumferential direction.

Computational Method

The computational method is summarized in Fig. 7. The governing equations are the Reynolds-averaged (or mass-averaged) Navier-Stokes equations. They are written here in conservation law form in two-dimensions. In this equation, U represents the conserved quantities: the density, momentum per unit volume in the x and y directions and the total energy per unit volume, and F and G are flux vectors associated with U in the x and y directions, respectively. The flux vectors contain the viscous stresses and the heat flux. These in turn are functions of the molecular and eddy viscosities. The value of the eddy viscosity used in the calculations will depend on the turbulence model employed. The calculations to be shown later will compare results obtained from some algebraic models for the eddy viscosity.

The numerical method employed is the latest implicit finite volume method of MacCormack (MacCormack, 1985). This is a stable, efficient, second order (in space) algorithm that utilizes flux splitting to take advantage of the direction information travels and is built around MacCormack's basic explicit second order accurate method (MacCormack, 1969).

No-slip and adiabatic boundary conditions are used at the surface of the trailing edge. Subsonic boundary conditions based on the method of characteristics are used at all the flow boundaries. At the inflow boundaries the total pressure, total temperature and the flow angle are specified. At the outflow boundary only the static pressure needs to be specified.

It was found that the specification of these boundary conditions for this subsonic flow problem was surprisingly critical to the results obtained. The flow boundary conditions are shown explicitly on Fig. 8 . Experimental values of p_t and T_t, taken from Spaid and Keener's data, were used where available at both inflow boundaries. Unfortunately these quantities were measured only in the boundary close to the body, both at the jet and at the X/C = 0.899 inflow station at the bottom of the trailing edge. It was assumed that T_t was a constant across the entire inflow boundaries. At these boundaries it was assumed that P_t varied linearly from the measured value at the edge of the boundary layer to

5

$P_{t\infty}$ at about 0.1 ft. off the body and remained constant for further distances.

The flow angle, $\tan^{-1} (v/u)$, is also needed at the inflow boundaries, but was not available. Therefore, this angle had to be approximated. At the top surface the flow angle is varied linearly from being parallel to the body at the surface to a value of zero at about 2 chords off of the surface. In the jet the flow angle is parallel to the top and bottom jet walls and varies linearly in between. The inflow angle off of the bottom surface was initially treated in the same manner as that off the top surface. However, in preliminary calculations these inflow angles were found to yield an unsatisfactory static pressure distribution at the inflow boundaries and the separation point moved to the bottom inflow boundary. For these calculations the static pressure at the outflow boundary was taken to be the tunnel static pressure. It was found that the location of the separation point could be moved toward the jet and the exit static pressure distributions on the inflow boundary made to agree better with the experimental results by varying the static pressure vertically from P_∞ at the top of the outflow boundary to 0.98 P_∞ at the bottom of the outflow boundary. It was also found that with the boundary conditions fixed, at values that gave reasonable results, that the results were sensitive to the distance that the outflow boundary was placed from the surface. Control volume radii of 2 ft and 3 ft were tried. Not having experimental evidence to guide either the choice of the inflow angle or the value of the outflow static pressure as a function of position it was decided to fix the static pressure at the outflow boundary to the nominal tunnel static pressure and to locate this boundary 2 feet (2.4 chords) off of the surface. It was also decided to vary the inflow angle along the lower inflow boundary as indicated by the short arrows on Fig. 8 . At the top of this boundary the flow angle is parallel to the surface. A linear variation was assumed from this upwash angle to a downwash angle of equal magnitude at a distant equal to 25% of chord below the body. Beyond this, the inflow angle was varied linearly to zero at 1 foot from the body and remained zero for the remaining distance. This tailoring of the inflow angle was done for a single turbulence model and yielded reasonable results. These boundary conditions remained fixed for all other turbulence models tested.

Since the results are indeed sensitive to the boundary conditions, it is apparent that to perform meaningful comparisons of turbulence models with experiment, measurements of flow field parameters need to be made in the boundary regions of the computational domain.

In the jet the total temperature was taken to be equal to the nominal total temperature of the tunnel and the total pressure was determined by matching the mass flow rate of the

experiment and assuming fully developed turbulent channel flow.

The computation is initiated by assuming no flow and a total pressure equal to the maximum P_t in the jet exists throughout the domain except for the exit boundary where the nominal tunnel static pressure is specified. From this the flow relaxes smoothly to a steady state.

Turbulence Models

Two basic algebraic eddy viscosity models were used in the calculations for this workshop. They are the well known Cebeci-Smith model and the more recent, but also well known Baldwin-Lomax model. Both are two layer models for the turbulence. Expressions for inner and outer regions of the boundary layer for both of these models are outlined on Fig. 9 . The Cebeci-Smith (C.S.) model is often inappropriate for complex flows because of great uncertainty in defining the boundary layer thickness δ and the displacement thickness δ^*. The Baldwin-Lomax (B.L.) model avoids this ambiguity by defining a length scale based on the location of the maximum of the velocity-function, F, of the vorticity, . For some complex flows the B.L. will also be inappropriate because F may have multiple maxima.

In the present calculations these two models were applied either without or with modifications.

The modifications to the B.L. model were as follows:

1. The history of the jet was included by evaluating the eddy viscosity at the exit plane of the jet using fully established channel flow relationships and length scales relative to the nearest wall. This jet-plane eddy viscosity was then blended with the local eddy viscosity through an exponential damping function W. The W was selected to vanish at X/C = 1.

2. The effect of curvature was included through the use of Bradshaw's curvature relation (Bradshaw, 1969). This relation is based on Bradshaw's analogy between streamline curvature and buoyancy. The R is the Richardson number.

3. To establish the effect of the intermittancy factor, I_{BL}, on the results, solutions were also obtained with I_{BL} set to unity. This was done to assure that the turbulence in the jet-free stream shear layer winded not be damped artificially through I_{BL}.

7

The boundary layer thickness used in the C.S. model was taken to be the distance normal to the surface where the velocity parallel to the surface was a maximum. For some parts of the trailing edge region the velocity increases monotonically with this distance and becomes unrealistically large. To avoid this the C.S. model was modified by not allowing to grow larger than 10 times the experimental value at the input boundary of the lower surface.

Results

The next seven figures show computation results obtained when these various turbulence models/modifications were applied to the trailing edge region of a circulation control airfoil under the conditions outlined earlier.

Fig. 10 shows a far field view of particle paths for one of the calculations. This is a typical result. Particle paths agree with streamlines in steady state flow. Here they represent the trajectory of particles selected at every fifth grid point along the inflow boundary. The dark band merely shows the coalescence of many particles that were selected close to the body.

In Fig. 11 a near field view of particle paths are presented for calculations based on the unmodified B. L. model and on this model with modifications for jet history, curvature and combined history and curvature. In these near field figures particle baths were initiated from every other grid point along the inflow boundary. All the results look similar overall. There is, however, evidence of a slight movement of the separation point toward the jet entrance when curvature or jet history effects are included in the turbulence model. This effect is more pronounced when the jet history and curvature terms are both included in the calculations.

The next two Figures (12 and 13) show the corresponding velocity vectors for each of the preceding particle path results. The length of the vectors shown here are proportional to the magnitude of the velocity. The vectors are placed at every third point circumferentially and every other point normal to the body. In spite of the small scale, the jet flow and flow above the jet lip are shown as distinct at the top inflow boundary. These two flows are seen to merge as fluid moves away from the jet. The jet also becomes less pronounced as it gives up its momentum to the mean flow. Also apparent on these figures is the merging of the flows from the top and bottom surface of the airfoil. All the velocity plots look similar and on close inspection reveal the separation points. The turbulence model with modifications for jet history and curvature is seen to predict separation to occur closest to the jet.

Figure 14 shows results obtained, for the same flow as in the previous figures, when the turbulence model is changed to the Cebeci-Smith model. In this figure particle paths and velocity vectors are shown for the unmodified and modified (δ limit) versions of the C.S. model discussed earlier. Both cases give similar results but the limit on has had the effect of moving the separation point closer to the jet. The velocity vectors for the two cases reveal differences that correspond to those seen between particle path comparisons.

The two basic turbulence models used in this study are compared in the next two figures. Figure 15, composed of the top half of Fig. 12 and the bottom half of Fig. 14, compares particle paths and velocity vectors for the B.L. and C.S. turbulence models. This comparison reveals that the basic flow patterns are considerably different for the two models. The location of the separation point is much closer to the jet for the C.S. than for the B.L. model. This is illustrated by the particle paths and the velocity vectors where the jet for the C.S. model is seen to leave the surface early and a reversed region profile is clearly visible below the jet about 45 degrees from the inlet line. Thus, this figure illustrates that the results obtained for this flow are very sensitive to the generic turbulence model used in the calculations.

To complete the comparisons of basic turbulence models and their modifications, the pressure distributions about the trailing edge are shown in Fig. 16. This comparison illustrates that there is not much difference between results obtained with the unmodified B.L. model and the B.L. model with jet history and curvature included. It also shows that large differences can occur between results obtained when the C.S. model is used in place of the B.L. model for fixed boundary conditions consistent with the latter model.

The differences in results between the two models (C.S. and B.L.) cannot be used to favor one over the other. They merely show that calculations for flow in the trailing edge region of a circulation control airfoil, with a single numerical scheme and fixed boundary conditions, are sensitive to the choice of the turbulence model. Recall that the boundary conditions were tailored to give reasonable results when the B.L. model was used in the calculations. Also, the results obtained with the B.L. model were very sensitive to the tailoring. Had the boundary conditions been tailored for the C.S. model the results shown on Fig. 16 would perhaps be very different.

Summary and Future Directions

In summary, a new, efficient, implicit algorithm for solving the two-dimensional Reynolds-averaged Navier-Stokes equations, with algebraic models of turbulence, has been

9

adapted to solve the trailing edge region of a circulation control airfoil.

The boundary conditions used at the entrance and exit regions of the entire control volume were found to be critically important. In future modeling experiments, it is critical that measurements of enough information be obtained to enable computations to have reliable and completely unambiguous boundary conditions.

Once boundary conditions were fixed, the numerical results were very dependent on the choice of the basic algebraic eddy viscosity model. Once a generic model had been chosen, however, results obtained from it were found to be insensitive to the modifications for streamwise curvature, jet history, itermittancy and outer length scales employed here.

In the future it is planned to incorporate higher order turbulence models into the code. These will include two-equation eddy viscosity models and, if needed, full stress transport models (HaMinh, et al, 1985). For efficiency some wall function development probably will be required (Viegas and Rubesin, 1985). The experimental data base for this modeling activity will include several boundary layer experiments with curved surfaces, and experiments in the vicinity of the trailing edge of circulation control airfoils, such as those of Novak and Cornelius (Novak and Cornelius, 1986). In addition, experiments such as the mean flow measurements of Spaid and Keener (Spaid and Keener, 1986) will be used to verify the results. It is also planned to interact with experimentalists here at NASA and elsewhere. Comparison calculations for various turbulence models would be done for these experiments and others as they become available. Eventually, the code could be extended to three-dimensions to study problems of real yawed wings.

References

Baldwin, B. and Lomax, H.: Thin-Layer Approximation and Algebraic Model for Separated Turbulent Flows, AIAA Paper No. 78-257, 1978.

Bradshaw, P.: The Analogy between Streamline Curvature and Buoyancy in Turbulent Shear Flow, J. Fluid Mech. Vol. 36, p. 177, 1969.

Cebeci, T. and Smith, A.M.O.: Analysis of Turbulent Boundary Layers, Academic Press, 1974, pp. 211-257.

HaMinh, H., Rubesin, M. W., Vandromme, D., and Viegas, J. R.: On the Use of Second Order Closure Modelling for the Prediction of Turbulent Boundary Layer/Shock Wave Interactions: Physical and Numerical Aspects, International Symposium on Computational Fluid Dynamics - Tokyo, Tokyo, Japan, Sept. 1985.

MacCormack, R. W.: The Effect of Viscosity in Hypervelocity Impact Cratering, AIAA Paper No. 69-354, 1969.

MacCormack, R. W.: Current Status of Numerical Solutions of the Navier-Stokes Equations, AIAA Paper No. 85-0032, 1985.

Novak, C. J. and Cornelius, K. C.: An LDV Investigation of a Circulation Control Airfoil Flowfield, AIAA Paper No. 86-0503, 1986.

Spaid, F. W. and Keener, E. R.: Boundary Layer and Wake Measurements on a Swept, Circulation-Control Wing, Circulation Control Workshop, NASA CP 2432, 1986. (Paper 11 of this compilation.)

Viegas, J. R. and Rubesin, M. W.: On the Use of Wall Functions as Boundary Conditions for Two-Dimensional Separated Compressible Flows, AIAA Paper No. 85-0180, 1985.

●Objective
●Identify turbulent modeling aspects
●Describe scope of current activities
●Briefly describe computation scheme
　　　* Grid
　　　* Governing equations
　　　* Numerical method
　　　* Turbulence models
●Examples——Applications of algebraic eddy viscosity
　　　models to the trailing edge of a circulation
　　　control wing
●Conclusions based on examples
●Future directions of research program

Fig. 1.- Purpose of the research program into turbulent flow prediction for circulation control airfoils.

To develop an improved turbulence model to permit the accurate computation of the flow fields about circulation control wings over a range of flight conditions and trailing edge configurations.

● Computations

● Experiments

Fig. 2.- Overall objective of research program.

- Three dimensionality

- Skewing effects

- Compressibility

- Merging of multiple streams

- Extreme streamwise curvature

- Separation

Fig. 3.- Modeling aspects of circulation control wings.

FLOW

SLOT

COMPUTATIONAL DOMAIN

EXPERIMENT
SPAID AND KEENER
$M_\infty = 0.426$
$P_{ti}/P_\infty = 1.4$
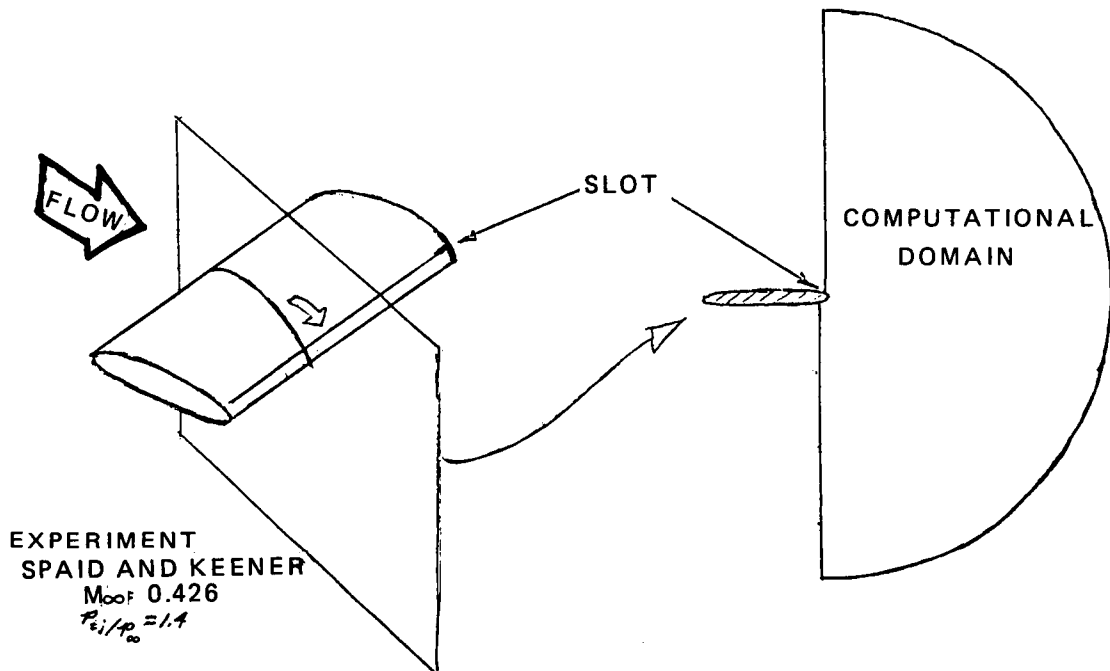
Fig. 4.- Computational domain for the trailing edge region of a circulation control wing.
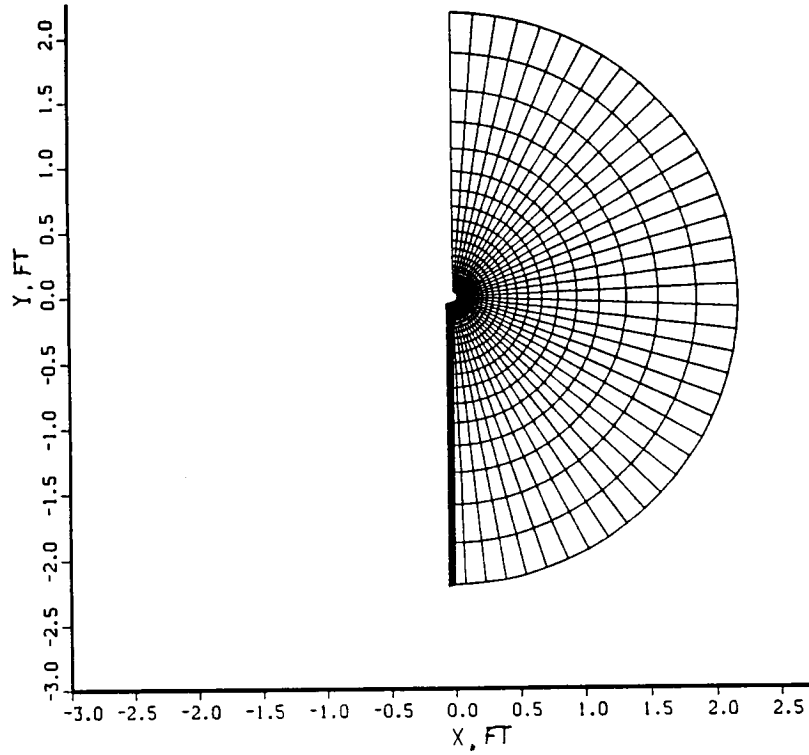
Fig. 5.- Far field grid used in the flow calculations.
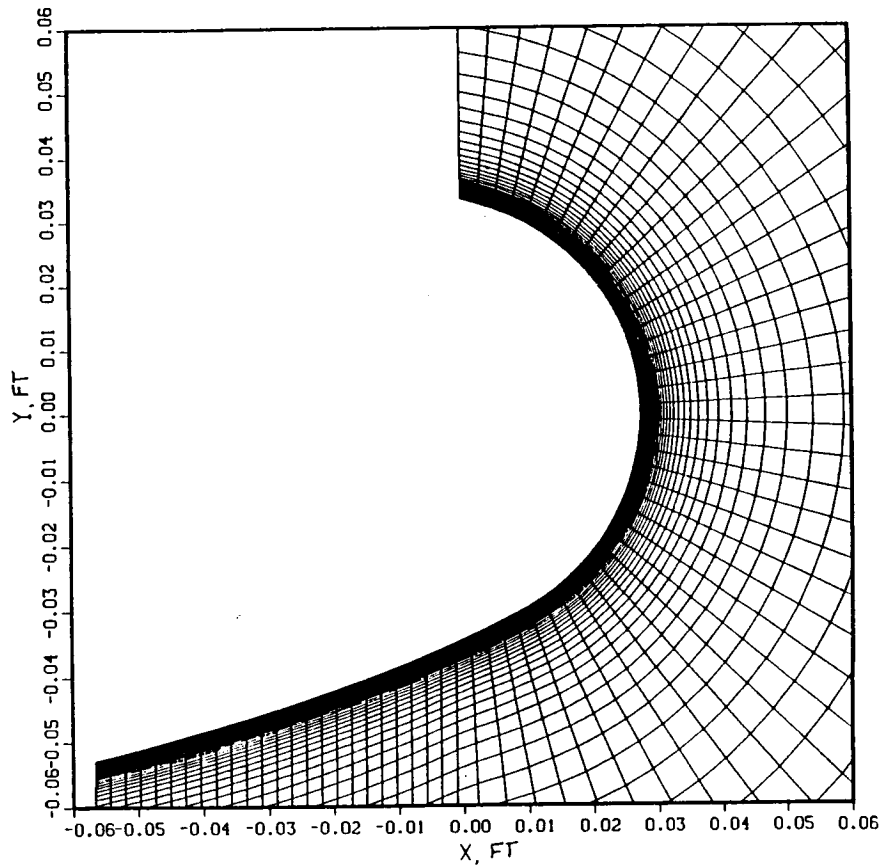
Fig. 6.- Magnified view of the grid showing the near field.

14

Governing Eqs. (Mass averaged Navier-Stokes equations)

$$\frac{\partial U}{\partial t} + \frac{\partial F}{\partial x} + \frac{\partial G}{\partial y} = 0$$

$$U = [\rho, \rho u, \rho v, \rho e]^T$$

F, G : flux vectors

$$F = \begin{bmatrix} \rho u \\ \rho u^2 + \sigma_{xx} \\ \rho u v - \tau_{xy} \\ u(\rho e + \sigma_{xx}) - v \tau_{xy} + q_x \end{bmatrix}$$

$$e = c_v T + (u^2 + v^2)/2$$

$$\sigma_x = p - 2(\mu + \mu_t)\left(\frac{\partial u}{\partial x} + \frac{1}{3} \operatorname{div} u\right)$$

$$\tau_{xy} = (\mu + \mu_t)\left(\frac{\partial u}{\partial y} + \frac{\partial v}{\partial x}\right)$$

$$q_x = -K_T \frac{\partial T}{\partial x}$$

Numerical Method.

    MacCormack : Implicit Finite Volume Method — 1985
        Basic Algorithm: Second order accurate explicit method
        Options: Implicit (including boundary conditions)
                Flux Splitting
                First or Second order accurate in Space,
                    first order in time.

Boundary Conditions:

    Surface : No slip , adiabatic

    Inflow: (Top and Bottom) Method of Characteristics
                         $P_t, T_t, \theta = v/u$, given

    Outflow : Method of Characteristics P (static) given

Fig. 7.- Summary of computational method.
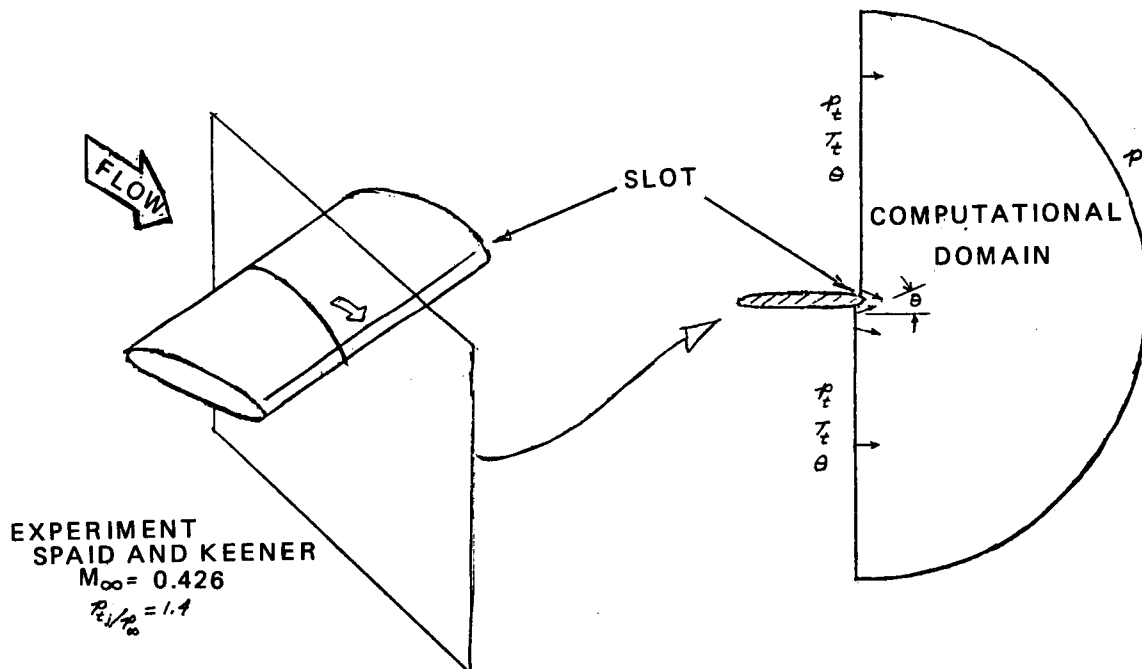
Fig. 8.- Computational domain for the trailing-edge region of a circulation control wing showing boundary conditions.

	Cebeci–Smith	Baldwin–Lomax

Inner region:

Cebeci–Smith: $\mu_{t_i} = \rho \ell^2 \left| \frac{\partial u}{\partial y} + \frac{\partial v}{\partial x} \right|$

Baldwin–Lomax: $\mu_{t_i} = \rho \ell^2 |\omega|$

Outer region:

Cebeci–Smith:
$$\mu_{t_o} = \bar{K} \rho u_e \delta^* / \mathcal{I}$$
$$\mathcal{I}, \mathcal{I}_{BL}, \text{ intermittency factors}$$
$$u_{diff}^2 = V_{max}^2 - V_{min}^2$$

Baldwin–Lomax:
the smaller of
$$\mu_{t_o} = \bar{K} \rho \, C_{cp} F_{max} Y_{max} / \mathcal{I}_{BL}$$
or
$$\mu_{t_o} = \bar{K} \rho \, C_{cp} C_{WK} \frac{y_{max} \, u_{diff}^2}{F_{max} \mathcal{I}_{BL}}$$
$$F = y|\omega|(1 - exp(-y/A))$$

Modifications:

History of jet $\mu_{t_i} = \mu_{t_j} W + \mu_{t_i}(1-W)$

Effect of curvature $\mu_{t_{c_i}} = \mu_{t_i} S^2 \qquad S = (1 + \beta R)^{-1}$

Limit tests on δ

Eliminate intermittancy

Fig. 9.- Expressions of inner and outer regions/for both models.
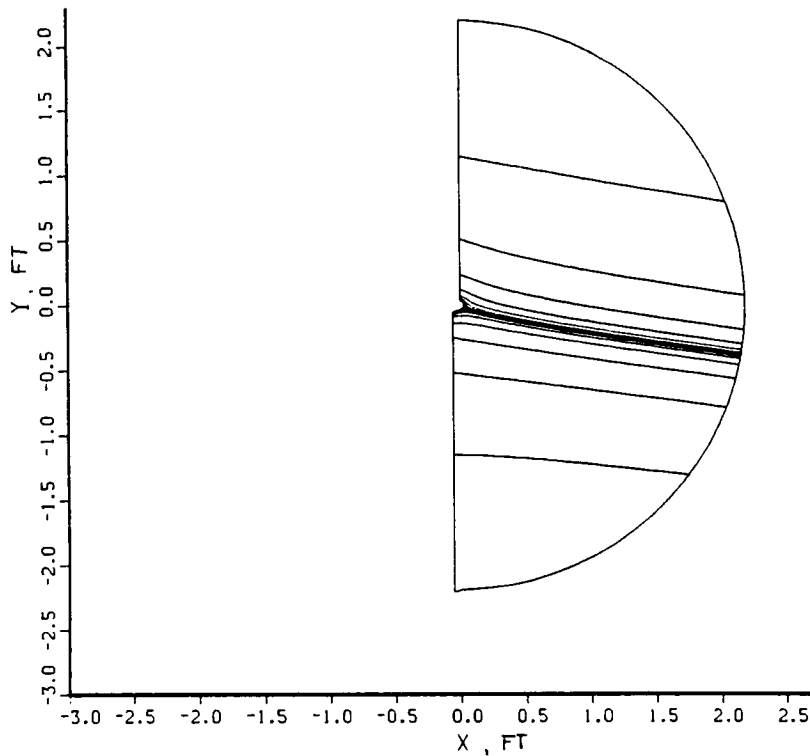
Fig. 10.- Example of far field view of particle path.
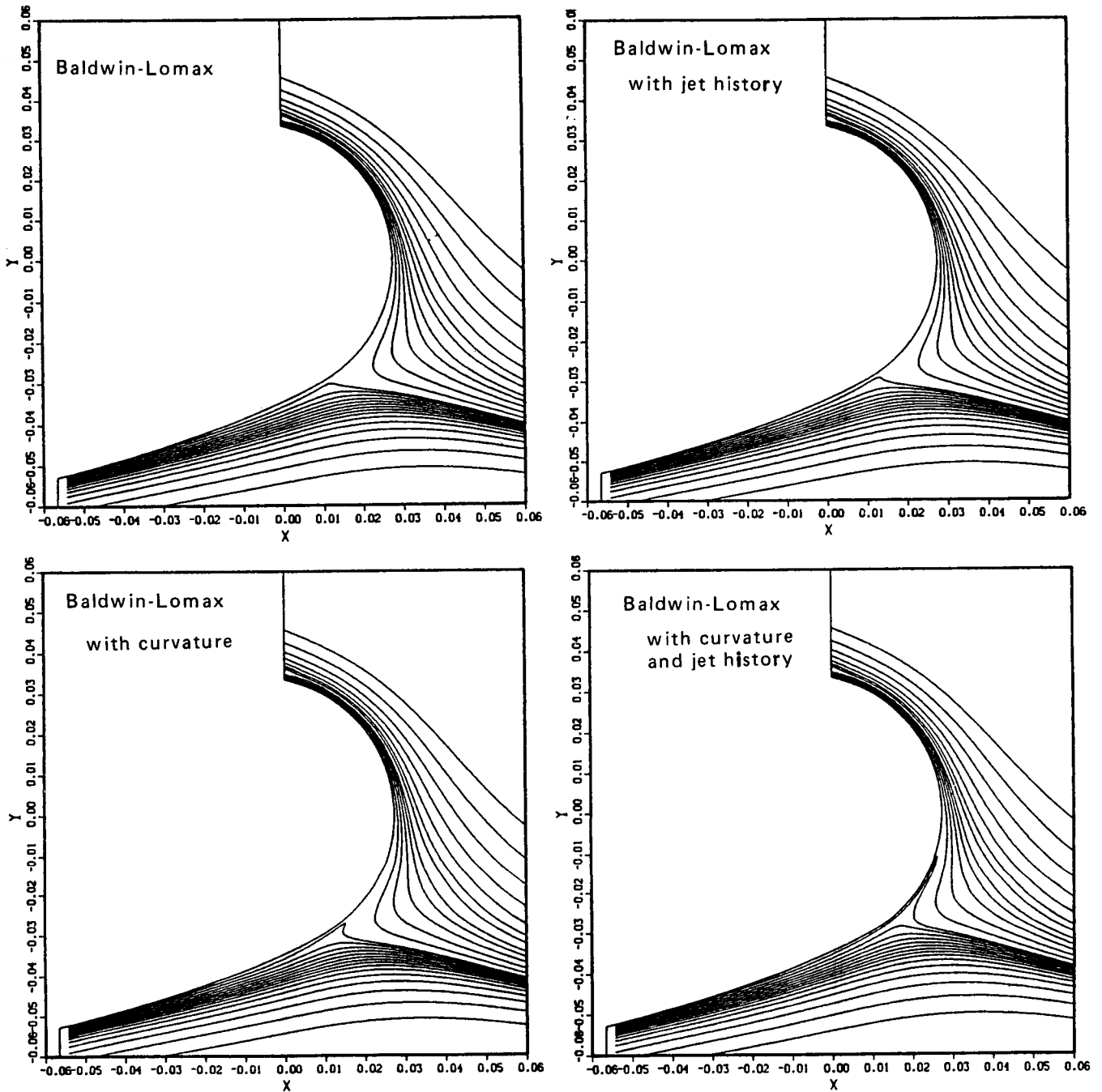
Fig. 11.- Near field view of particle paths for calculations based on
Baldwin-Lomax model.

PARTICLE PATHS   VELOCITY VECTORS
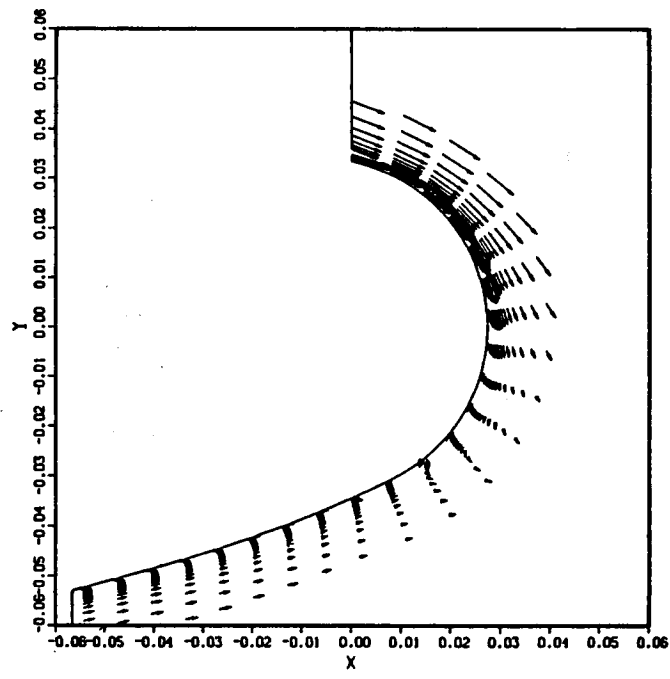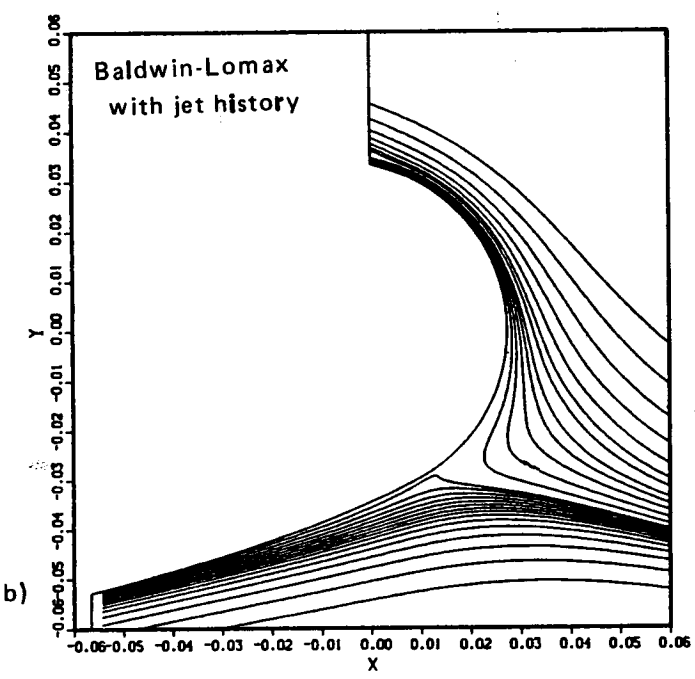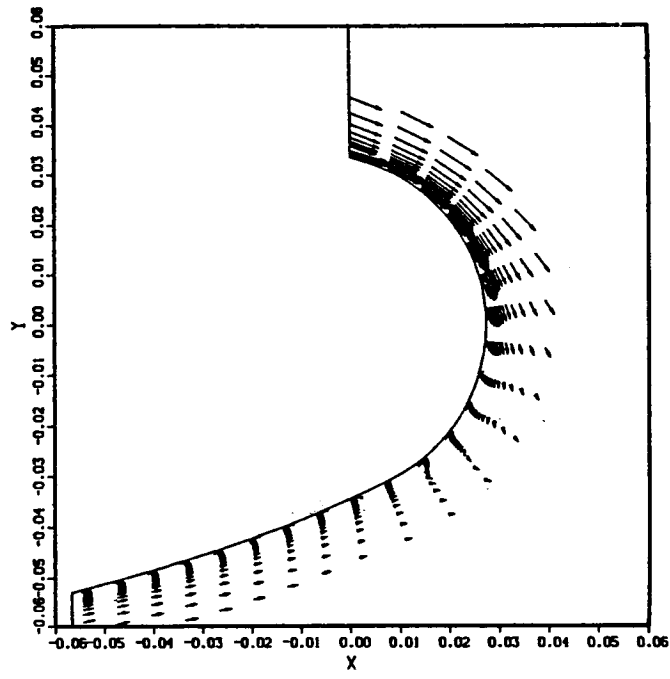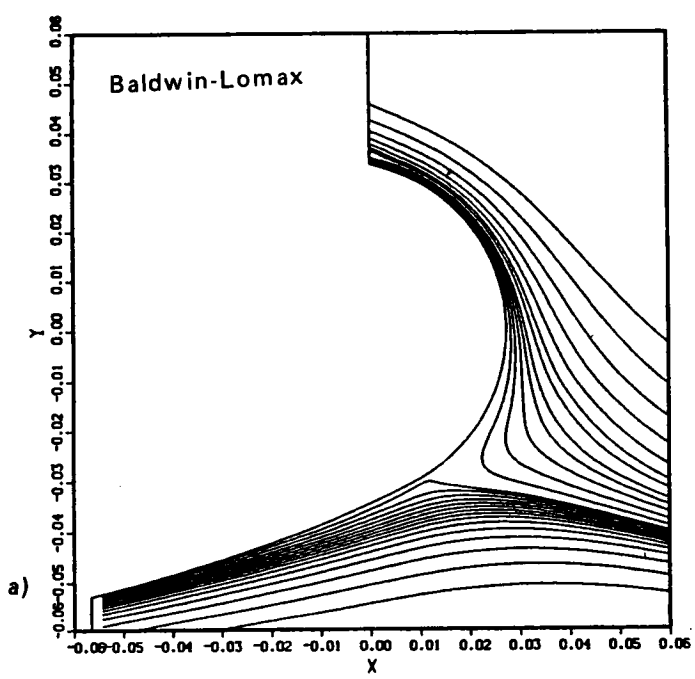
Fig. 12.- Particle paths and corresponding velocity vectors. a) Baldwin-Lomax
model; b) Baldwin-Lomax model with jet history.

18

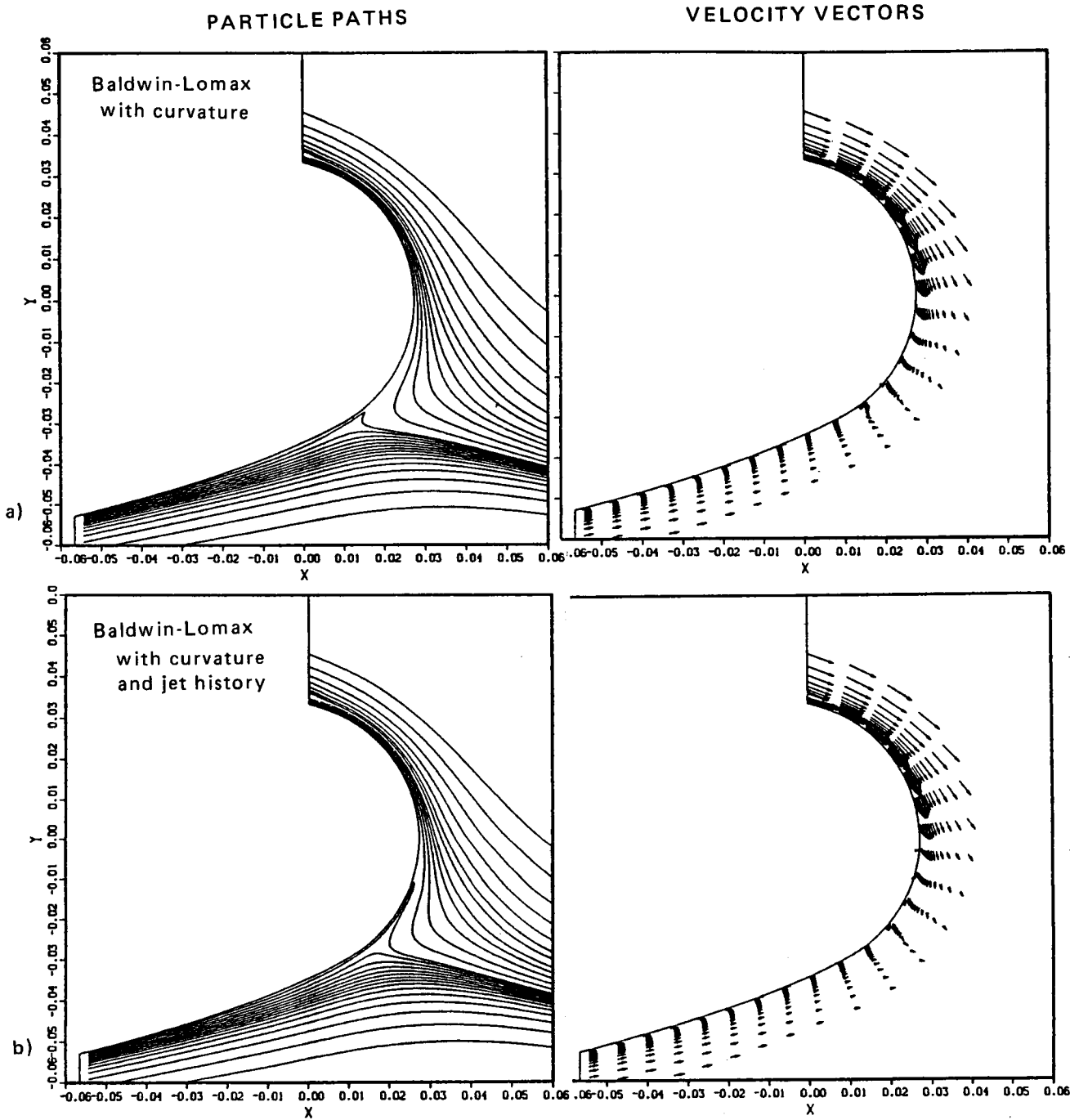PARTICLE PATHS   VELOCITY VECTORS
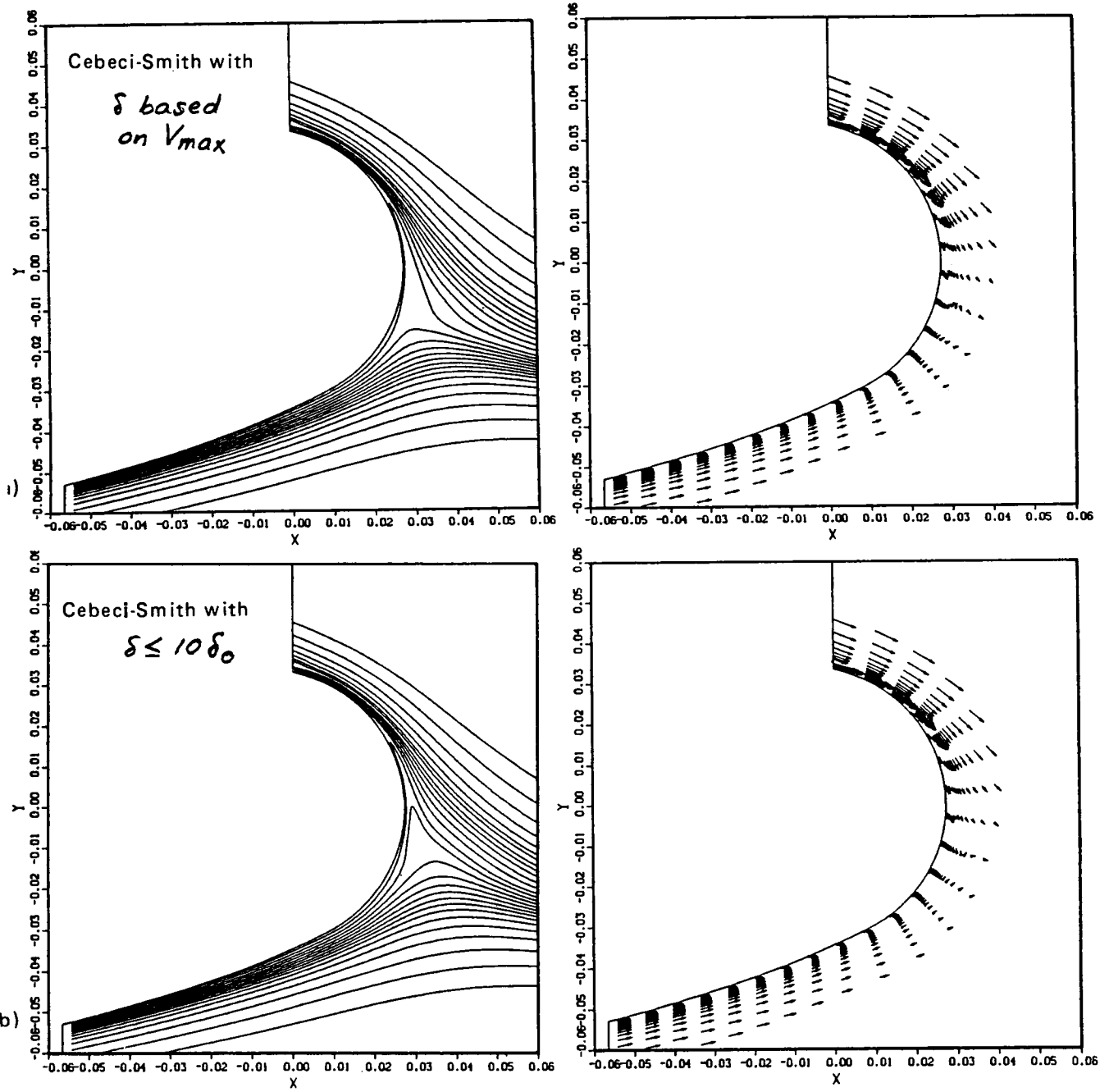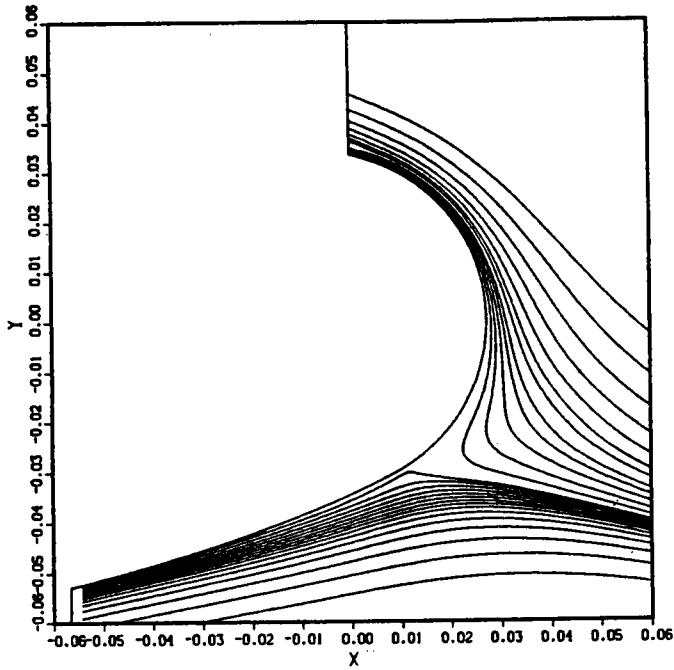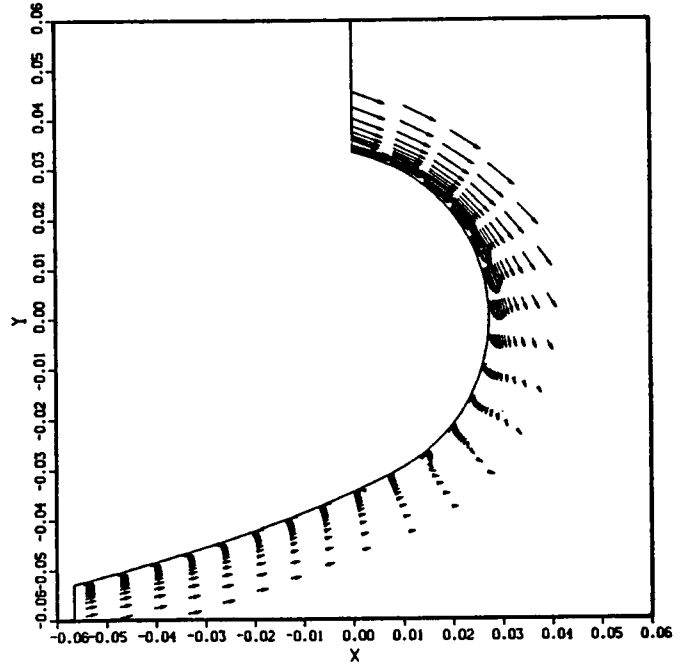

Fig. 13.- Particle paths and corresponding velocity vectors. a) Baldwin-Lomax with curvature; b) Baldwin-Lomax with curvature and jet history.

Fig. 14.- Particle paths and corresponding velocity vectors using the Cebeci-Smith model. a) δ based on V_{max}; b) $\delta \leq 10\ \delta_o$

BALDWIN-LOMAX
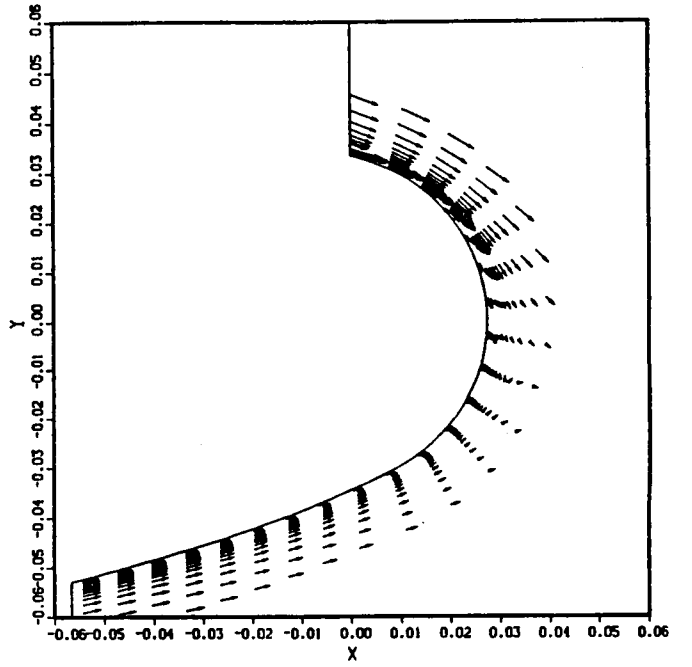
PARTICLE PATHS   VELOCITY VECTORS

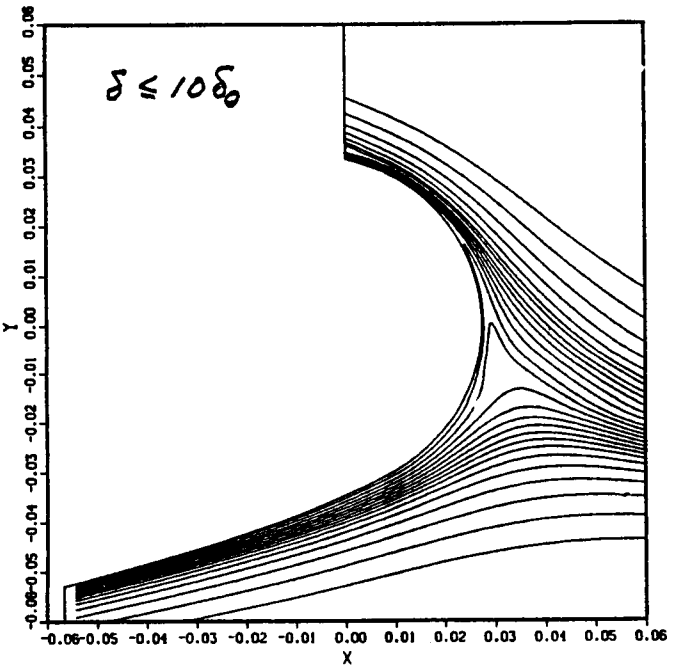CEBECI-SMITH

$\delta \leq 10\delta_0$

Fig. 15.- Comparison of near region flow fields obtained using Baldwin-Lomax and Cebeci-Smith models.
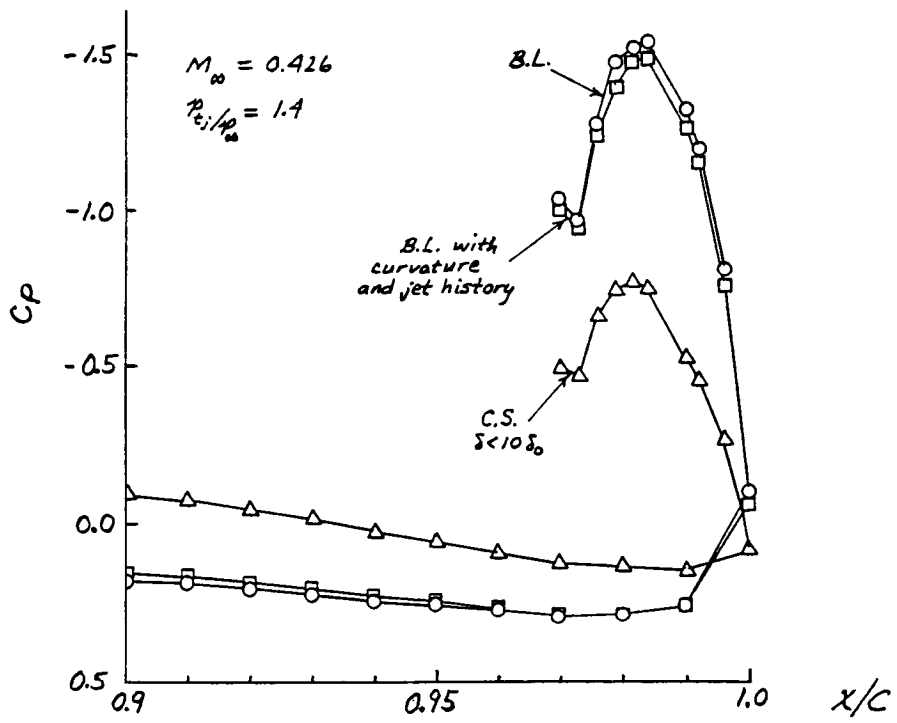
21

Fig. 16.- Comparison of both models based on pressure distribution about the trailing edge.